Determinants of α-Conotoxin BuIA Selectivity on the Nicotinic Acetylcholine Receptor β Subunit†

David L. Shiembob,‡ Ryan L. Roberts,‡ Charles W. Luetje,§ and J. Michael McIntosh*,‡,||

Department of Biology, University of Utah, Salt Lake City, Utah, Molecular and Cellular Pharmacology, Miller School of Medicine, University of Miami, Miami, Florida, and Department of Psychiatry, University of Utah, Salt Lake City, Utah

Received June 12, 2006; Revised Manuscript Received July 12, 2006

ABSTRACT: Neuronal nicotinic acetylcholine receptors (nAChRs) are pentamers composed of α and β subunits. Different molecular compositions of these subunits constitute various receptor subtypes that are implicated in the pathophysiology and/or treatment of several disease states but are difficult to distinguish pharmacologically. α-Conotoxins are a group of small, structurally defined peptides that may be used to molecularly dissect the nAChR-binding site. Heteromeric nAChRs generally contain either a β2 or β4 subunit in addition to an α subunit at the ligand-binding interface. α-Conotoxin BuIA kinetically distinguishes between β2- and β4-containing nAChRs, with long off times for the latter. Mutational studies were used to assess the influence of residues that line the putative acetylcholine-binding pocket but differ between β2 and β4 subunits. Residues Thr/Lys59, Val/Ile111, and Phe/Gln119 of the respective β2 and β4 subunits are critical to off-rate differences. Among these residues, Thr59 of nAChR β2 may interfere with effective access to the binding site, whereas Lys59 may facilitate this binding.

Nicotinic acetylcholine receptors (nAChRs)[1] are involved in numerous physiological central nervous system (CNS) functions including learning and memory, reward, analgesia, and motor control. These nAChRs are present not only postsynaptically but also on presynaptic and preterminal sites, where stimulation activates the synaptic release of neurotransmitters including dopamine, norepinephrine, serotonin, glutamate, and γ-aminobutyric acid (*1*). The ability to modulate the release of these key neurotransmitters has led to proposals that nicotinic drugs are potential novel therapeutics for the treatment of a broad array of maladies including cognitive dysfunction, addiction, pain, and Parkinson's disease, as well as psychotic, mood, and anxiety disorders (for a review, see ref *2*).

nAChRs are pentamers made up of α and β subunits; different combinations of these subunits constitute subtypes of receptors that have discrete anatomical distributions. To date, all neuronal nAChRs that contain an α2, α3, α4, or α6 subunit also contain and require a β2 or β4 subunit to function. The presence of either the β2 and/or β4 subunit influences pharmacological properties of the nAChR, such as agonist efficacy, desensitization kinetics, and Ca^{+2} permeability (*3*). Competitive nicotinic ligands generally bind to both the α and β subunit that together form a ligand-binding interface. There is considerable conservation of residues that form the ligand-binding sites of nAChR subtypes, contributing to the challenge of designing selective drugs (*4*). Further, complicating matters is the fact that the nAChR fluctuates among different states, including (at least) resting, active, and desensitized (*5*). A practical consequence of this is that binding selectivity may not translate into functional selectivity. For instance, the antagonist A-186253 has 200 000-fold binding selectivity for α4β2 versus α7 nAChRs yet shows only 20-fold selectivity with respect to the functional block of these receptor subtypes (*6*). The rational design of functionally selective ligands must, therefore, take into account the allosteric nature of the nAChR function.

Conotoxins are a large family of peptide ligands from carnivorous mollusks of the genus *Conus*. Cocktails of these peptides are used to envenomate fish and other prey. Identified macromolecular targets include a broad array of ligand- and voltage-gated ion channels and G-protein-coupled receptors (*7*, *8*). Because of their pharmacological specificity, some of these peptides are being developed as medications (*9*, *10*). ω-Conotoxin MVIIA (ziconotide) is a potent analgesic that blocks N-type calcium channels and is in current clinical use (*11*). Contulakin-G (CGX-1160) is a neurotensin type-I receptor agonist in phase-I human clinical trials for spinal cord injury pain (*12*). Xen2174, an analogue of MrIA, is an allosteric blocker of the norepinephrine transporter in phase-I clinical trials for treatment of cancer pain (*13*). α-Conotoxin Vc1.1 is a nAChR antagonist in phase-I human clinical trials for neuropathic pain (*14*, *15*). Thus, understanding the mechanism by which conotoxins achieve their target specificity is a priority.

α-Conotoxins are two disulfide bridge small peptides that target to and are widely used as structural probes of nAChRs

† This work was supported by the National Institutes of Health Grants MH53631 (J.M.M.) and DA08102 (C.W.L.). D.L.S. and R.L.R. also received partial support from the University of Utah Bioscience Undergraduate Research Program.

* To whom correspondence should be addressed: University of Utah, Department of Biology, 257 South 1400 East, Salt Lake City, UT 84112-0840. Telephone: 801-585-3622. Fax: 801-585-5010. E-mail: mcintosh.mike@gmail.com.

‡ Department of Biology, University of Utah.

§ University of Miami.

|| Department of Psychiatry, University of Utah.

[1] Abbreviations: nAChR, nicotinic acetylcholine receptor; ACh, acetylcholine; CI, 95% confidence interval.

10.1021/bi0611715 CCC: $33.50
Published on Web 08/25/2006

(*16*). The crystal structure of the *Lymnae* acetylcholine (ACh) binding protein bound to α-conotoxin PnIA (A10L D14K), a blocker of α7 nAChRs, was solved and indicates that this α-conotoxin binds with high affinity to a structure homologous to the resting state of the nAChR (*17*). Recently, a novel peptide with unique selectivity features was identified from *Conus bullatus* (*18*). In this paper, we have investigated nAChR β subunit residues present at the ligand-binding interface that profoundly affect the kinetics of the block by this ligand known as α-conotoxin BuIA. Among these, Lys59 may allow for more effective access to the high-affinity binding site.

MATERIALS AND METHODS

Chemical Synthesis. α-Conotoxin BuIA was synthesized on a Fmoc amide resin using Fmoc chemistry and standard side protection, except on cysteine residues. Cys residues were protected in pairs with *S*-trityl on Cys1 and Cys3 (the first and third cysteine residues) and *S*-acetamidomethyl on Cys2 and Cys4. The peptide was removed from the resin and precipitated. A two-step oxidation protocol was used to selectively fold the peptides as described previously (*18*).

Mutagenesis of Receptors. The notation used for point mutants is to list the naturally occurring residue, followed by its position, followed by the change made. For example, β2T59G is a β2 subunit with the 59 position threonine replaced by a glycine. Point mutants were constructed using the QuikChange site-directed mutagenesis kit (Stratagene). The mutant receptors were in either the pGEMHE vector (Liman, E. R., Tytgat, J., Hess, P. (1992) *Neuron*, 861−871.) or the pSP65 vector (Promega). All (PCR) mutations were confirmed by sequencing.

Electrophysiology. Oocytes were harvested and injected with cRNA encoding nAChR subunits as described previously (*19*). All clones were from rat. For off-rate kinetics, a 30 μL cylindrical oocyte recording chamber fabricated from Sylgard was gravity-perfused with ND96A (96.0 mM NaCl, 2.0 mM KCl, 1.8 mM $CaCl_2$, 1.0 mM $MgCl_2$, 1 μM atropine, and 5 mM HEPES at pH 7.1−7.5) at a rate of ∼2 mL/min. All toxin solutions also contained 0.1 mg/mL bovine serum albumin to reduce nonspecific adsorption of the peptide. ACh-gated currents were obtained with a two-electrode voltage-clamp amplifier (model OC-725B, Warner Instrument, Hamden, CT), and data were captured as previously described (*20*). The membrane potential of the oocytes was clamped at −70 mV. To apply a pulse of ACh to the oocyte, the perfusion fluid was switched to one containing ACh for 1 s. This was automatically done at intervals of 1 min. The ACh was diluted in ND96A. For control responses, the ACh pulse was preceded by perfusion with ND96A. The concentration of ACh was 100 μM. Toxin was bath-applied for 5 min, followed by a pulse of ACh. The volume of entering ACh is such that the toxin concentration remains at a level >50% of that originally in the bath until the ACh response has peaked (<2 s). Thereafter, toxin was washed away, and subsequent ACh pulses were given every 1 min, unless otherwise indicated. All ACh pulses contain no toxin, because it was assumed that little if any bound toxin washed away in the brief time (in less than 2 s that it takes for the responses to peak). In our recording chamber, the bolus of ACh does not project directly at the oocyte but rather enters tangentially, swirls, and mixes with the bath solution.

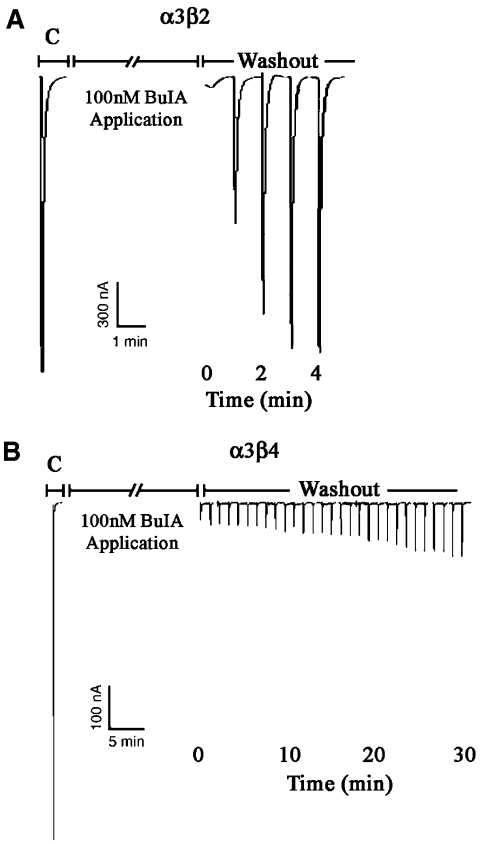

FIGURE 1: α-Conotoxin BuIA has slow washout kinetics for α3β4 versus α3β2 nAChRs. Toxin (100 nM) was applied to oocytes expressing α3β2 nAChRs (A) and α3β4 nAChRs (B). After a 5 min incubation, toxin was washed out and responses to a 1 s pulse of ACh were measured every 1 min. C, control response to ACh prior to the addition of the toxin.

For determination of the toxin on-rate and when longer than 5 min of toxin application was needed to reach the maximum block, toxin was applied by continuous perfusion to the oocytes as previously described (*21*). When the on-rate was rapid, ACh was applied every 1 min, but 15 s time intervals were determined by staggering the start time of these 1 min intervals in 15 s increments and then combining the data. The average peak amplitude of three control responses just preceding exposure to toxin was used to normalize the amplitude of each test response to obtain a "percent response" or "percent block". Each data point of a dose−response curve represents the average value ± standard error (SE) of measurements from at least three oocytes.

RESULTS

α-Conotoxin BuIA blocks both β2*[2] and β4* nAChRs. However, the off-rate from αxβ4* nAChRs is much slower than that of αxβ2 nAChRs (*18*). An example of this difference for rat α3β2 versus α3β4 nAChRs is shown in Figure 1.

Data from X-ray crystallography, receptor labeling, mutagenesis, and receptor modeling based on the molluscan ACh-binding protein indicate that the ACh-binding pocket is constituted by a hydrophobic cage of conserved aromatic residues from both the α and β subunits in proximity to the two disulfide-linked vicinal cysteines in loop C of the α

[2] The asterisk indicates the presence of additional subunits.

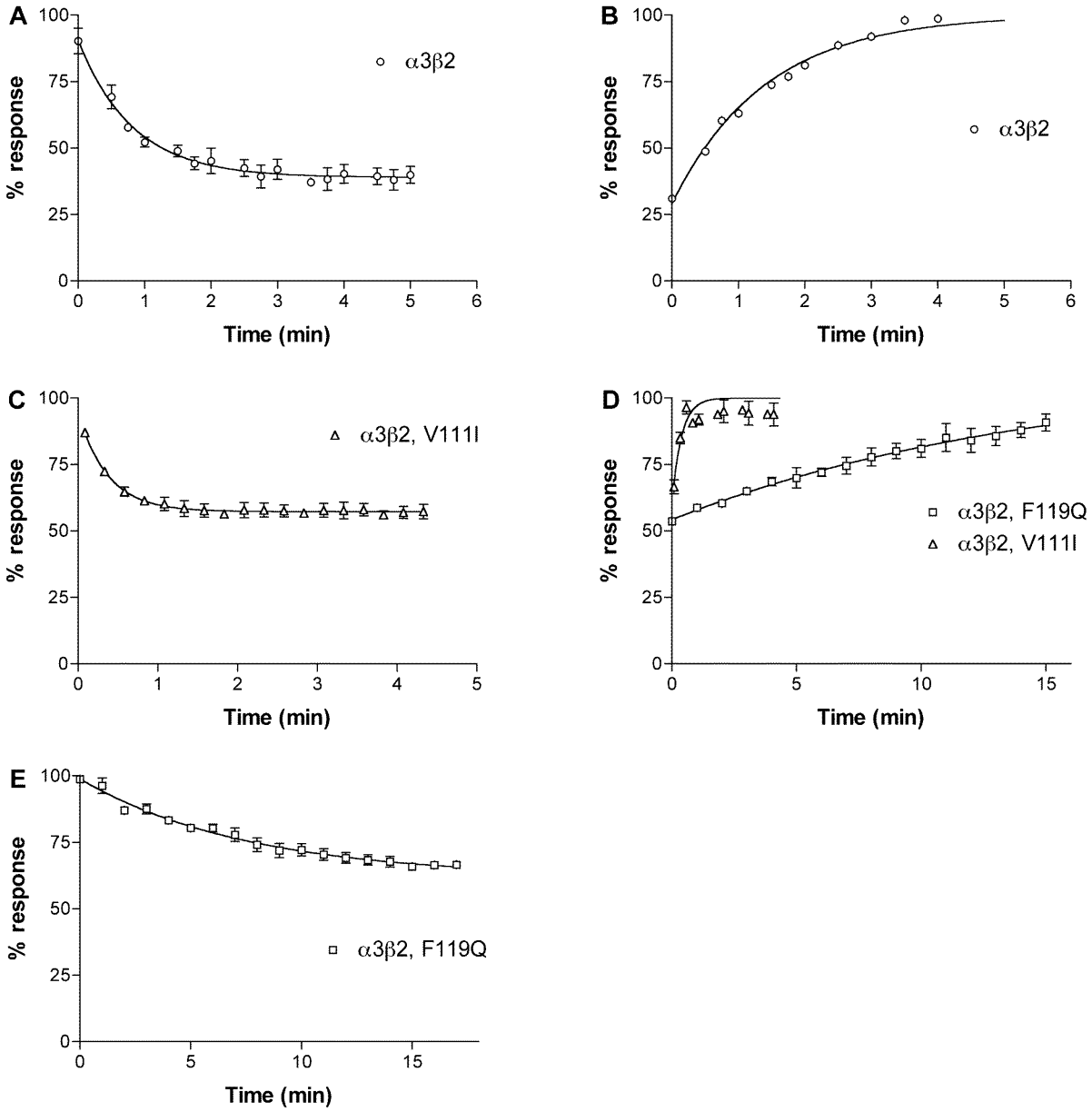

FIGURE 2: Kinetics of the block of α-conotoxin BuIA on α3β2 and α3 with point mutations in β2. Note that β2 Val111Ile speeds recovery, whereas Phe119Gln slows recovery from the block by α-conotoxin BuIA. (A) α-Conotoxin BuIA (5 nM) applied to α3β2. (B) Washout of α-conotoxin BuIA from α3β2. (C) α-Conotoxin BuIA (6 nM) applied to α3β2Val111Ile. (D) Washout of α-conotoxin BuIA from α3β2Val111Ile and α3β2Phe119Gln. (E) α-Conotoxin BuIA (500 pM) applied to α3β2Phe119Gln. Toxin was applied by perfusion to oocytes expressing the indicated nAChRs as described in the Materials and Methods. Response to a 1 s pulse of ACh was measured. Results are summarized in Table 1.

Table 1: α-Conotoxin BuIA Kinetic Constants for the Block of α3β2 nAChRs[a]

	k_{on} (min^{-1} M^{-1})	k_{off} (min^{-1})	k_i (M)	IC_{50} (M)
α3β2	1.12 (0.19−2.05) × 10^8	0.656 (0.483−0.829)	5.85 × 10^{-9}	5.72 × 10^{-9}[b]
α3β4[b]	4.68 (3.06−6.30) × 10^5	0.0111	2.38 × 10^{-8}	2.77 × 10^{-8}
α3β2,V111I	5.21 (0−18.2) × 10^7	2.614 (1.58−3.64)	4.91 × 10^{-8}	8.98 (7.6−10.6) × 10^{-9}
α3β2,F119Q	1.05 (0.864−1.24) × 10^8	0.0936 (0.0813−0.106)	8.91 × 10^{-10}	7.35 (5.92−9.13) × 10^{-10}
α3β2,T59D	6.72 (2.19−11.3) × 10^7	0.0448 (0.0274−0.0622)	6.65 × 10^{-10}	5.66 (5.00−6.40) × 10^{-10}
α3β2,T59G	1.17 (0.26−2.08) × 10^8	0.0581 (0.0489−0.0660)	5.01 × 10^{-10}	3.62 (2.15−6.08) × 10^{-10}
α3β2,T59K	6.03 (5.34−6.72) × 10^7	0.0178 (0.0164−0.0192)	2.95 × 10^{-10}	2.43 (1.86−3.19) × 10^{-10}
α3β2,T59S	2.83 (1.71−3.94) × 10^7	0.0878 (0.0636−0.112)	3.11 × 10^{-10}	4.93 (4.30−5.68) × 10^{-10}
α3β2,T59V	1.61 (1.08−2.14) × 10^8	0.301 (0.259−0.343)	1.87 × 10^{-9}	1.08 (0.993−1.18) × 10^{-9}

[a] Numbers in parentheses are 95% confidence intervals (CIs). [b] Values are from ref *18*.

subunit (*3*, *5*). The conservation of these residues among nAChR subtypes restricts the ability of ligands to discriminate among these subtypes. However, nonconserved residues appear to line the binding pocket and could allow for ligand subtype specificity (*17*, *22*). Three residues in β2, Val111, Phe119, and Leu121, form a hydrophobic partial rim around

the binding pocket. Val111 is replace by Ile in β4, and Phe119 is replaced by Gln in β4. We therefore tested these residues to assess their role in the kinetics of the block by α-conotoxin BuIA. Substitution of Val with Ile (β2 Val111Ile) led to an increase in k_{off} (Figure 2 and Table 1). Because of the fast kinetics, measuring k_{obs} and k_{off} was difficult. To ensure that we had obtained reliable measurements, we used a second method to determine kinetic constants. k_{obs} was plotted versus the toxin concentration according to the equation $k_{obs} = k_{on}(F) + k_{off}$, where F is the free toxin concentration, the slope is k_{on}, and the y intercept is k_{off}. Using this method, we found k_{on} to be 5.995×10^7 min^{-1} M^{-1} and k_{off} to be 2.446 min^{-1} (data not shown), giving a k_i of 4.08×10^{-8} M in good agreement with values determined by the methods shown in Figure 2 and detailed in Table 1. This k_i value is 4.5-fold higher than the IC_{50}, which may represent the error associated with calculating k_{on} when k_{obs} is approximately equal to k_{off}. In contrast to the results with Val111Ile, substitution of the hydrophilic Gln for Phe (β2 Phe119Gln) led to a 7-fold decrease in k_{off}, partially explaining the longer off time of α-conotoxin BuIA for α3β2 versus α3β4 nAChRs. The k_{on} for β2 Phe119Gln was not significantly different than wild-type β2. Results for both mutations are shown in Table 1 and Figure 2.

β2 Thr59 is located at the opposite edge of the binding pocket rim. This residue is replaced by a positively charged Lys in β4. Kinetics of the unblock for this mutation were difficult to quantitate because of the very long on and off times (Figure 3) combined with limitations of oocyte recording duration and a tendency for the ACh response to drift over time. Kinetics were therefore also assessed by determining the k_{obs} at four different toxin concentrations (Figure 3C). In this instance, accuracy is hindered by the uncertainty of the y intercept where the error includes the ordinate. Despite these technical limitations, the k_i values calculated by the two methods are in reasonable agreement, 2.95×10^{-10} versus 3.81×10^{-10} M, respectively. The mutation β2 Thr59Lys had a large effect upon decreasing the k_{off} of α-conotoxin BuIA (36.9-fold) compared to a less than 2-fold decrease in k_{on}.

α-Conotoxin MII is a peptide with an α 4/7 structure whose nAChR selectivity profile is functionally distinct from that of α-conotoxin BuIA (*23*). It was previously reported that the mutation β2Thr59Lys decreased the affinity of α-conotoxin MII. We therefore examined what effects the Thr59Lys mutation had on the kinetics of binding α-conotoxin MII. In contrast to α-conotoxin BuIA, the Thr59Lys affected k_{on} but had no effect on k_{off} (Figure 4 and Table 2).

Because the mutation β2 Thr59Lys had the most profound effect on α-conotoxin BuIA off-rates, we further investigated the role of position 59 in leading to the substantial difference in k_{off} for α-conotoxin BuIA, by creating additional position 59 point mutations in the β2 subunit. The concentration response analysis of α-conotoxin BuIA on the various point mutants in shown in Figure 5 and Table 3, and data on toxin kinetics are shown in Figure 6 and Table 3. Thr has an aliphatic hydroxyl side chain. Nonconservative substitution of Thr59 by Gly, which has only a hydrogen atom side chain, surprisingly also led to a large decrease in the α-conotoxin BuIA k_{off} (11.3-fold) and a 15.1-fold decrease in k_i. Similarly, substitution of β2 Thr59 with a negatively charged residue, Asp, also led to a large decrease (14.6-fold) in α-conotoxin BuIA k_{off} as well as an 11.4-fold decrease in k_i. Thus, nonconservative substitution of Thr by Lys, Gly, or Asp leads to an increase in affinity in each instance. These results suggest that the primary effect of Thr59 in the β2 subunit is to interfere with α-conotoxin BuIA binding. Such a result might be explained by steric hindrance by Thr but not Lys, Gly, or Asp. Thr is the only residue in this set that has a side chain that is branched at the β carbon. We reasoned that this branching could be a source of steric hindrance to toxin binding and, if so, that replacement of Thr with Val

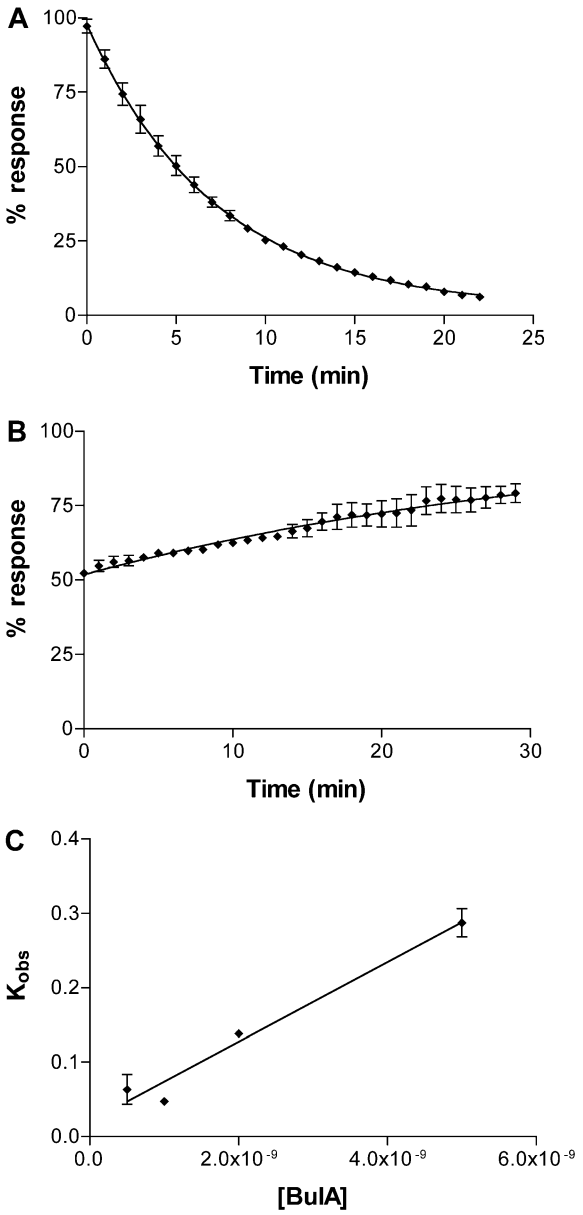

FIGURE 3: Kinetics of the block of α-conotoxin BuIA on α3β2Thr59Lys. (A) α-Conotoxin BuIA (2 nM) perfusion applied to α3β2Thr59Lys. The response to ACh was measured every 1 min. (B) Washout of α-conotoxin BuIA. (C) Plot of the observed on-rate versus the toxin concentration. Toxin (500 pM, 1 nM, 2 nM, and 5 nM) was applied by perfusion to oocytes expressing α3β2Thr59Lys as described in the Materials and Methods. Response to a 1 s pulse of ACh was measured. Kinetics constants were calculated according to the equation $k_{obs} = k_{on}(F) + k_{off}$, where F is the free toxin concentration and the y intercept $= k_{off}$. Using this equation, $k_{on} = 5.36 \pm 0.67 \times 10^7$ min^{-1} M^{-1} and $k_{off} = 0.0204 \pm 0.018$ min^{-1}.

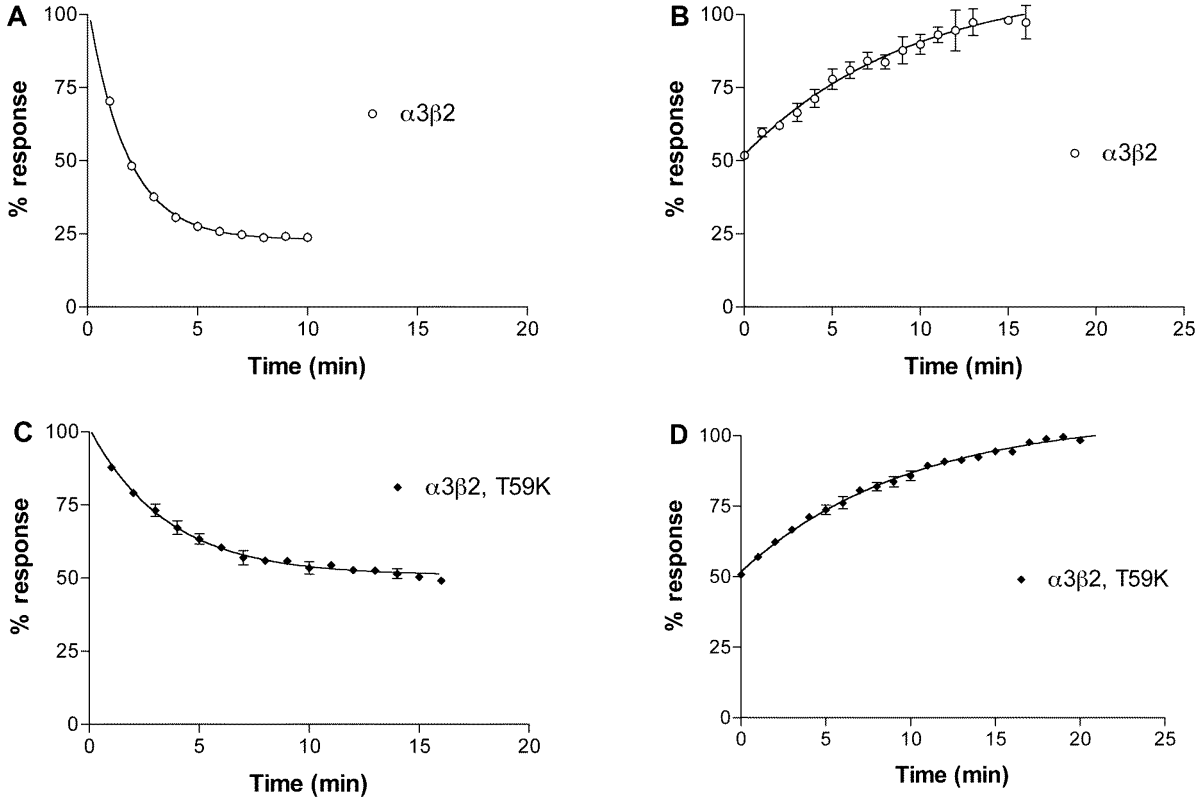

FIGURE 4: Kinetics of the block of α-conotoxin MII on α3*β*2Thr59Lys. Note that the Thr59Lys mutation affects k_{on} but not k_{off}. (A) α-Conotoxin MII (10 nM) applied to α3*β*2. (B) Washout of α-conotoxin MII from α3*β*2 nAChRs. (C) α-Conotoxin MII (10 nM) applied to α3*β*2Thr59Lys. (D) Washout of α-conotoxin MII from α3*β*2Thr59Lys. Toxin was applied by perfusion to oocytes expressing α3*β*2Thr59Lys as described in the Materials and Methods. Response to a 1 s pulse of ACh was measured. Results are summarized in Table 2.

Table 2: α-Conotoxin MII Kinetic Constants for the Block of α3*β*2 nAChRs[a]

	k_{on} (min^{-1} M^{-1})	k_{off} (min^{-1})	k_i (M)
α3*β*2	4.61 (3.78−5.42) × 10^7	0.106 (0.0565−0.156)	2.32 × 10^{-9}
α3*β*2,T59K	1.80 (1.30−2.32) × 10^7	0.102 (0.0847−0.119)	5.65 × 10^{-9}

[a] Numbers in parentheses are CIs.

(an aliphatic hydrophobic residue, branched at the *β* carbon) would, like Thr, also hinder binding. Indeed, this is the case; substitution of *β*2 Thr59 by Val caused only a relatively modest change (2.18-fold decrease) in k_{off} compared to Thr. In contrast, Ser normally acts as a conservative substitution for Thr. Both Ser and Thr have polar −OH groups in their side chain and differ by only a single methyl group. However, unlike Thr, Ser is not branched at the *β* carbon. The results indicate that the replacement of Thr with Ser leads to a larger change (7.46-fold decrease) in k_{off}. It will be of future interest to compare receptor position 59 Leu versus Ile to further examine the effects of branching at the *β* carbon.

DISCUSSION

In this study, we have investigated the kinetics of the functional block of nAChRs by α-conotoxin BuIA. These kinetics are dependent upon the *β* nAChR subunit; the *β*4 subunit but not the *β*2 subunit is associated with a slow recovery from the toxin block. Residues 59 and 119 of the rat *β* subunit are shown to be key determinants of this aspect of toxin action.

Two hydrophobic residues that line the *β*2-subunit-binding cleft were initially examined. Phe119 in *β*2 is Gln in *β*4, and Val111 in *β*2 is Ile in *β*4. The effects of these two residue changes are opposite. When Phe119 of *β*2 is replaced by Gln, there is a decrease in α-conotoxin BuIA k_{off}, leading to a 6.6-fold increase in toxin affinity. When *β*2 V111 is replaced by Ile, there is both an increase in k_{off} as well as a decrease in k_{on}, leading to an 8.3-fold decrease in toxin affinity. The largest change occurs when *β*2 Thr59 is substituted with Lys that is in the homologous position of *β*4. There is a 37-fold decrease in k_{off} partially offset by a 1.9-fold decrease in k_{on}, producing a 19.8-fold increase in affinity.

Thr59 has been documented as a positive determinant of high-affinity binding for certain competitive antagonists of nAChRs. Changing *β*2Thr59 to Lys as it occurs in *β*4 caused a 9-fold *decrease* in sensitivity to dihydro-*β*-erythroidine and a 71-fold *decrease* in sensitivity to *κ*-bungarotoxin (*24*) (see Table 3). This change in the nAChR also led to a small (2−4-fold) *decrease* in sensitivity of the block by the 4/7 α-conotoxin MII (ref *25* and this paper). In the present work, we show that this decrease for α-conotoxin MII is due to a decrease in the binding *on-rate* of MII. Significantly, the situation for BuIA is opposite. That is, a change from Thr59 to Lys59 leads to a 20-fold *increase* in sensitivity to the toxin block, because of a substantial *decrease* in k_{off}.

Thus, the decrease in k_{off} of α-conotoxin BuIA for α3*β*4 compared to α3*β*2 nAChRs can be largely explained by the decrease in k_{off} seen in the *β*2 Thr59Lys and Phe119Gln

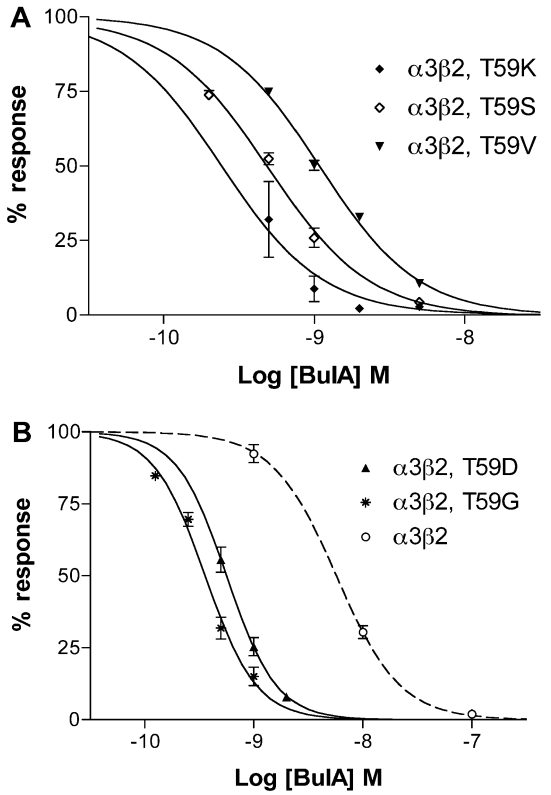

FIGURE 5: Concentration response analysis of α-conotoxin BuIA on α3β2 nAChRs with point mutations in position 59 of β2. Toxin was applied by perfusion to oocytes expressing nAChRs as described in the Materials and Methods. Results are summarized in Table 1. The dashed line shows the wild-type α3β2 data from ref *18*.

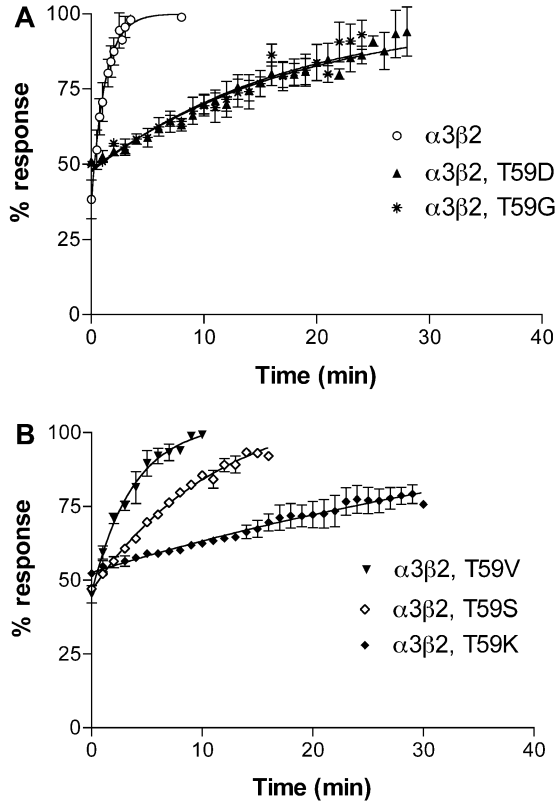

FIGURE 6: Recovery from the block by α-conotoxin BuIA of α3β2 nAChRs with point mutations in position 59 of β2. Response to a 1 s pulse of ACh was measured every 1 min after toxin washout. Results are summarized in Table 1.

Table 3: Effect of β2 Thr59Lys[a]

toxin	α3β2 IC_{50} (nM)	α3β2 T59K IC_{50} (nM)	ratio[b]	α3β2 k_{off} (min^{-1})	α3β2 T59K k_{off} (min^{-1})	ratio[c]
DHβE	410[d]	3800[d]	9.27			
κ-BTx	1.7[d]	120[d]	70.6			
α-CTx MII	3.5[e]	14[e]	4.00	0.106	0.102	1.039
α-CTx BuIA	5.72	0.243	0.0425	0.656	0.0178	.0271

[a] DHβE, dihydro-β-erythroidine; κ-BTx, κ-bungarotoxin; α-CTx, α-conotoxin. [b] (α3β2 T59K IC_{50})/(α3β2 IC_{50}). [c] (α3β2 T59K k_{off})/(α3β2 T59K k_{off}). [d] Data are from ref *32*. [e] Data are from ref *25*.

mutations, partially offset by the increase in k_{off} observed in the Val111Ile mutation. However, given that residue differences can cause either increases or decreases in the α-conotoxin k_{off}, the present data do not exclude the contribution of other subunit residues to the long α-conotoxin off times observed for β4-containing nAChRs. The slow recovery from the α-conotoxin BuIA block has been demonstrated for α3β4 versus α3β2 nAChR subtypes in different species, including rat, mouse, and human (*18*). Position 59 and 111 differences between β2 and β4 subunits are conserved among rat, mouse, and human. In position 119, the β2 residues are conserved, whereas β4 is Gln in rat and mouse but is Leu in human (Figure 7).

Cryoelectron microscopy images of the *Torpedo* nAChR have led to near atomic-scale resolution of this muscle nAChR (*26*, *27*), and the molluscan ACh-binding protein has provided a valuable crystal structure for homology modeling of neuronal nAChRs (*28*). Modeling of the α3β2 nAChR based on this structure (*29*) shows β2 Thr59 at the edge of a cleft believed to be the ACh-binding pocket (Figure 8). The present results are consistent with α-conotoxin BuIA acting as an antagonist by preventing the access of ACh to this binding pocket. The results further suggest that Lys59 (present in the homologous position of the β4 subunit) may allow for better access of the toxin to the binding cavity. Such increased access may lead to a more favorable interaction with receptor residues. Although a more favorable interaction could come by either increased k_{on} and/or decreased k_{off}, in the case of α-conotoxin BuIA binding, the improvement comes almost entirely from the latter. Thus, residue 59 appears to be situated at a critical location on the β portion of the α/β nAChR subunit interface. Previously studied toxins, including alkaloids (dihydro-β-erythroidine from the seeds of the trees and shrubs of the genus *Erythrina*), proteins (κ-bungarotoxin from the Tawainese banded krait, *Bungarus multicinctus*) and peptides (α-conotoxin MII from the marine snail *Conus*), may bind to β2 Thr59, and the replacement of Thr59 with Lys decreases the affinity for these ligands. In contrast, the replacement of Thr59 with residues with widely varying physicochemical properties in each instance leads to an increase in the affinity for α-conotoxin BuIA.

The α-conotoxins are two disulfide loop peptides that may be structurally grouped according to loop size (*30*). Docking simulations of the 4/7 family of α-conotoxins (4 residues in loop 1 and 7 residues in loop 2) suggest that these toxins bind at a cleft located at one entrance to the ACh-binding site and above the β9/β10 hairpin (*22*, *31*). The recent crystal

```
                                10                  20                  30                  40                  50
Rat Beta 2          T D T E E R L V E H L L D P S R Y N K L I R P A T N G S E L V T V Q L M V S L A Q L I S V H E R E Q
Mouse Beta 2        T D T E E R L V E H L L D P S R Y N K L I R P A T N G S E L V T V Q L M V S L A Q L I S V H E R E Q
Human Beta 2        T D T E E R L V E H L L D P S R Y N K L I R P A T N G S E L V T V Q L M V S L A Q L I S V H E R E Q
Rat Beta 4          A N A E E K L M D D L L N K T R Y N N L I R P A T S S S Q L I S I R L E L S L S Q L I S V N E R E Q
Mouse Beta 4        A N A E E K L M D D L L N K T R Y N N L I R P A T S S S Q L I S I R L E L S L S Q L I S V N E R E Q
Human Beta 4        A N A E E K L M D D L L N K T R Y N N L I R P A T S S S Q L I S I K L Q L S L A Q L I S V N E R E Q

                          D
                    60                  70                  80                  90                  100
Rat Beta 2          I M T T N V W L T Q E W E D Y R L T W K P E D F D N M K K V R L P S K H I W L P D V V L Y N N A D G
Mouse Beta 2        I M T T N V W L T Q E W E D Y R L T W K P E D F D N M K K V R L P S K H I W L P D V V L Y N N A D G
Human Beta 2        I M T T N V W L T Q E W E D Y R L T W K P E E F D N M K K V R L P S K H I W L P D V V L Y N N A D G
Rat Beta 4          I M T T S I W L K Q E W T D Y R L A W N S S C Y E G V N I L R I P A K R V W L P D I V L Y N N A D G
Mouse Beta 4        I M T T S I W L K Q E W T D Y R L A W N S S C Y E G V N I L R I P A K R V W L P D I V L Y N N A D G
Human Beta 4        I M T T N V W L K Q E W T D Y R L T W N S S R Y E G V N I L R I P A K R I W L P D I V L Y N N A D G

                          E
                    110                 120                 130                 140                 150
Rat Beta 2          M Y E V S F Y S N A V V S Y D G S I F W L P P A I Y K S A C K I E V K H F P F D Q Q N C T M K F R S
Mouse Beta 2        M Y E V S F Y S N A V V S Y D G S I F W L P P A I Y K S A C K I E V K H F P F D Q Q N C T M K F R S
Human Beta 2        M Y E V S F Y S N A V V S Y D G S I F W L P P A I Y K S A C K I E V K H F P F D Q Q N C T M K F R S
Rat Beta 4          T Y E V S V Y T N V I V R S N G S I Q W L P P A I Y K S A C K I E V K H F P F D Q Q N C T L K F R S
Mouse Beta 4        T Y E V S V Y T N V I V R S N G S I Q W L P P A I Y K S A C K I E V K H F P F D Q Q N C T L K F R S
Human Beta 4        T Y E V S V Y T N L I V R S N G S V L W L P P A I Y K S A C K I E V K Y F P F D Q Q N C T L K F R S

                          F
                    160                 170                 180                 190                 200
Rat Beta 2          W T Y D R T E I D L V L K S D V A S L D D F T P S G E W D I I A L P G R R N E N P D D S T Y V D
Mouse Beta 2        W T Y D R T E I D L V L K S D V A S L D D F T P S G E W D I I A L P G R R N E N P D D S T Y V D I T
Human Beta 2        W T Y D R T E I D L V L K S E V A S L D D F T P S G E W D I V A L P G R R N E N P D D S T Y V D I T
Rat Beta 4          W T Y D H T E I D M V L K S P T A I M D D F T P S G E W D I V A L P G R R T V N P Q D P S Y V D V T
Mouse Beta 4        W T Y D H T E I D M V L K S P T A I M D D F T P S G E W D I V A L P G R R T V N P Q D P S Y V D V T
Human Beta 4        W T Y D H T E I D M V L M T P T A S M D D F T P S G E W D I V A L P G R R T V N P Q D P S Y V D V T
```

FIGURE 7: Alignment of the N-terminal extracellular domains (preceding transmembrane I) of β2 and β4 nAChR subunits. Residue positions (59, 111, and 119) tested in this study are indicated with dots. Bars indicate the agonist-binding domain loops D, E, and F. The locations of the loops are taken from ref *5*.

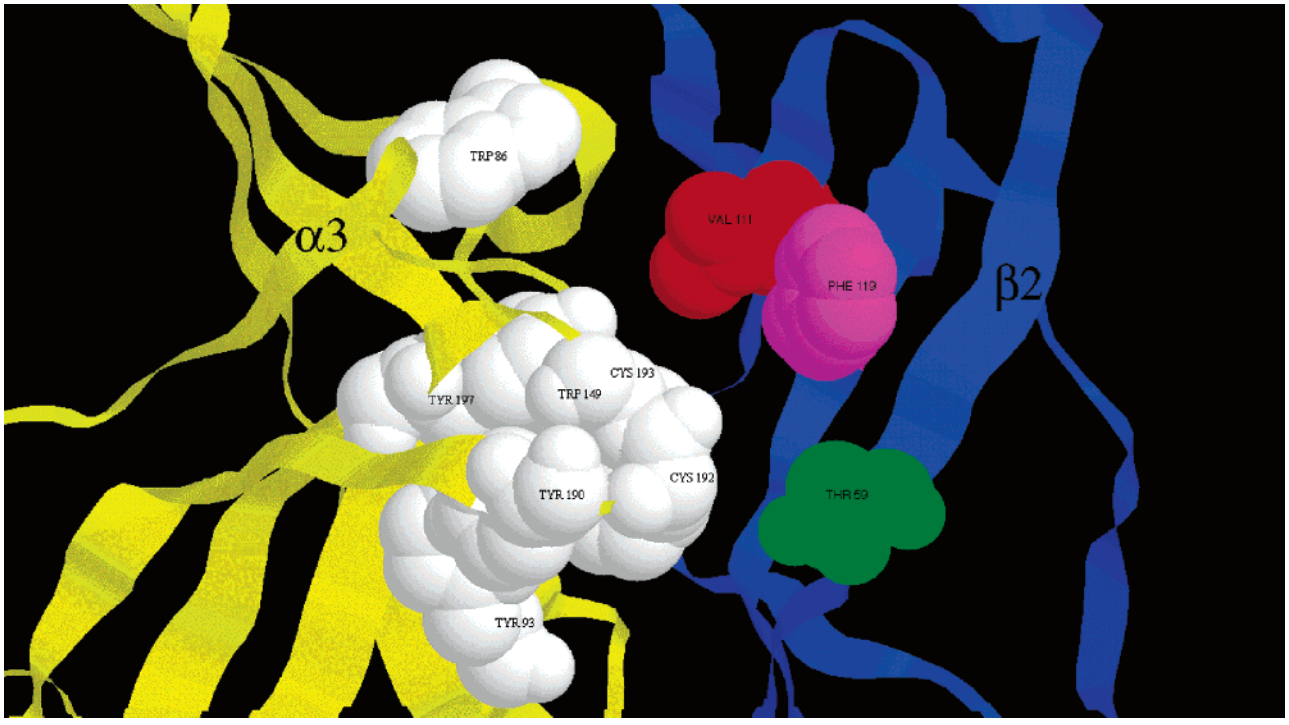

FIGURE 8: α3β2 nAChR-binding site. The ACh-binding site at an α3/β2 interface is shown within a model of the 3β2 extracellular domain. Proposed α3 subunit agonist-binding residues (*33*) are shown in white space filling. Residues affecting α-conotoxin BuIA binding kinetic differences between β2 and β4 subunits are shown in color space filling.

structure of a 4/7 α-conotoxin analogue bound to the *Lymnae* ACh-binding protein is consistent with this binding mode (*17*). Residues Thr59, Val111, Phe119, and Leu121 line this cleft (Figure 8). Only residue, Leu121, is conserved between the β2 and β4 nAChR subunits; Leu121 is also found in a homologous position in δ, γ, and ϵ subunits as well as the (−) face of the α7 subunit. Thus, Thr59, Val111, and Phe119 but not Leu121 represent potential residues that may be exploited to achieve discrimination between β2- and β4-containing nAChRs.

ACKNOWLEDGMENT

We thank Greg Bulaj for helpful discussions.

REFERENCES

1. Wonnacott, S. (1997) Presynaptic nicotinic ACh receptors, *Trends Neurosci. 20*, 92−98.
2. Gotti, C., and Clementi, F. (2004) Neuronal nicotinic receptors: From structure to pathology, *Prog. Neurobiol. 74*, 363−396.
3. Jensen, A. A., Frolund, B., Liljefors, T., and Krogsgaard-Larsen, P. (2005) Neuronal nicotinic acetylcholine receptors: Structural revelations, target identifications, and therapeutic inspirations, *J. Med. Chem. 48*, 4705−4745.
4. Gotti, C., Riganti, L., Vailati, S., and Clementi, F. (2006) Brain neuronal nicotinic receptors as new targets for drug discovery, *Curr. Pharm. Des. 12*, 407−428.
5. Corringer, P. J., Le Novere, N., and Changeux, J.-P. (2000) Nicotinic receptors at the amino acid level, *Annu. Rev. Pharmacol. Toxicol. 40*, 431−458.
6. Itier, V., Schonbachler, R., Tribollet, E., Honer, M., Prinz, K., Marguerat, A., Bertrand, S., Bunnelle, W. H., Schubiger, P. A., Meyer, M. D., Sullivan, J. P., Bertrand, D., and Westera, G. (2004) A-186253, a specific antagonist of the $\alpha4\beta2$ nAChRs: Its properties and potential to study brain nicotinic acetylcholine receptors, *Neuropharmacology 47*, 538−557.
7. Terlau, H., and Olivera, B. M. (2004) *Conus* venoms: A rich source of novel ion channel-targeted peptides, *Physiol. Rev. 84*, 41−68.
8. Lewis, R. J. (2004) Conotoxins as selective inhibitors of neuronal ion channels, receptors and transporters, *IUBMB Life 56*, 89−93.
9. Livett, B. G., Gayler, K. R., and Khalil, Z. (2004) Drugs from the sea: Conopeptides as potential therapeutics, *Curr. Med. Chem. 11*, 1715−1723.
10. Layer, R. T., and McIntosh, J. M. (2006) Conotoxins: Therapeutic potential and application, *Mar. Drugs 4*, 119−142.
11. Miljanich, G. P. (2004) Ziconotide: Neuronal calcium channel blocker for treating severe chronic pain, *Curr. Med. Chem. 11*, 3029−3040.
12. Craig, A. G., Norberg, T., Griffin, D., Hoeger, C., Akhtar, M., Schmidt, K., Low, W., Dykert, J., Richelson, E., Navarro, V., Macella, J., Watkins, M., Hillyard, D., Imperial, J., Cruz, L. J., and Olivera, B. M. (1999) Contulakin-G, an O-glycosylated invertebrate neurotensin, *J. Biol. Chem. 274*, 13752−13759.
13. Sharpe, I. A., Palant, E., Schroeder, C. I., Kaye, D. M., Adams, D. J., Alewood, P. F., and Lewis, R. J. (2003) Inhibition of the norepinephrine transporter by the venom peptide χ-MrIA. Site of action, Na^+ dependence, and structure−activity relationship, *J. Biol. Chem. 278*, 40317−40323.
14. Lang, P. M., Burgstahler, R., Haberberger, R. V., Sippel, W., and Grafe, P. (2005) A *Conus* peptide blocks nicotinic receptors of unmyelinated axons in human nerves, *NeuroReport 16*, 479−483.
15. Sandall, D. W., Satkunanathan, N., Keays, D. A., Polidano, M. A., Liping, X., Pham, V., Down, J. G., Khalil, Z., Livett, B. G., and Gayler, K. R. (2003) A novel α-conotoxin identified by gene sequencing is active in suppressing the vascular response to selective stimulation of sensory nerves in vivo, *Biochemistry 42*, 6904−6911.
16. Nicke, A., Wonnacott, S., and Lewis, R. J. (2004) α-Conotoxins as tools for the elucidation of structure and function of neuronal nicotinic acetylcholine receptor subtypes, *Eur. J. Biochem. 271*, 2305−2319.
17. Celie, P. H., Kasheverov, I. E., Mordvintsev, D. Y., Hogg, R. C., van Nierop, P., van Elk, R., van Rossum-Fikkert, S. E., Zhmak, M. N., Bertrand, D., Tsetlin, V., Sixma, T. K., and Smit, A. B. (2005) Crystal structure of nicotinic acetylcholine receptor homolog AChBP in complex with an α-conotoxin PnIA variant, *Nat. Struct. Mol. Biol. 12*, 582−588.
18. Azam, L., Dowell, C., Watkins, M., Stitzel, J. A., Olivera, B. M., and McIntosh, J. M. (2005) α-Conotoxin BuIA, a novel peptide from *Conus bullatus*, distinguishes among neuronal nicotinic acetylcholine receptors, *J. Biol. Chem. 280*, 80−87.
19. Cartier, G. E., Yoshikami, D., Gray, W. R., Luo, S., Olivera, B. M., and McIntosh, J. M. (1996) A new α-conotoxin which targets $\alpha3\beta2$ nicotinic acetylcholine receptors, *J. Biol. Chem. 271*, 7522−7528.
20. Luo, S., Kulak, J. M., Cartier, G. E., Jacobsen, R. B., Yoshikami, D., Olivera, B. M., and McIntosh, J. M. (1998) α-Conotoxin AuIB selectively blocks $\alpha3\beta4$ nicotinic acetylcholine receptors and nicotine-evoked norepinephrine release, *J. Neurosci. 18*, 8571−8579.
21. Luo, S., Nguyen, T. A., Cartier, G. E., Olivera, B. M., Yoshikami, D., and McIntosh, J. M. (1999) Single-residue alteration in α-conotoxin PnIA switches its nAChR subtype selectivity, *Biochemistry 38*, 14542−14548.
22. Dutertre, S., and Lewis, R. J. (2004) Computational approaches to understand α-conotoxin interactions at neuronal nicotinic receptors, *Eur. J. Biochem. 271*, 2327−2334.
23. McIntosh, J. M., Azam, L., Staheli, S., Dowell, C., Lindstrom, J. M., Kuryatov, A., Garrett, J. E., Marks, M. J., and Whiteaker, P. (2004) Analogs of α-conotoxin MII are selective for $\alpha6$-containing nicotinic acetylcholine receptors, *Mol. Pharmacol. 65*, 944−952.
24. Harvey, S. C., Maddox, F. N., and Luetje, C. W. (1996) Multiple determinants of dihydro-β-erythroidine sensitivity on rat neuronal nicotinic receptor α subunits, *J. Neurochem. 67*, 1953−1959.
25. Harvey, S. C., McIntosh, J. M., Cartier, G. E., Maddox, F. N., and Luetje, C. W. (1997) Determinants of specificity for α-conotoxin MII on $\alpha3\beta2$ neuronal nicotinic receptors, *Mol. Pharmacol. 51*, 336−342.
26. Miyazawa, A., Fujiyoshi, Y., Stowell, M., and Unwin, N. (1999) Nicotinic acetylcholine receptor at 4.6 Å resolution: Transverse tunnels in the channel wall, *J. Mol. Biol. 288*, 765−786.
27. Unwin, N., Miyazawa, A., Li, J., and Fujiyoshi, Y. (2002) Activation of the nicotinic acetylcholine receptor involves a switch in conformation of the α subunits, *J. Mol. Biol. 319*, 1165−1176.
28. Brejc, K., van Dijk, W. J., Klaassen, R. V., Schuurmans, M., van der Oost, J., Smit, A. B., and Sixma, T. K. (2001) Crystal structure of an ACh-binding protein reveals the ligand-binding domain of nicotinic receptors, *Nature 411*, 269−276.
29. Everhart, D., Reiller, E., Mirzoian, A., McIntosh, J. M., Malhotra, A., and Luetje, C. W. (2003) Identification of residues that confer α-conotoxin PIA sensitivity on the $\alpha3$ subunit of neuronal nicotnic acetylcholine receptors, *J. Pharmacol. Exp. Ther. 306*, 665−670.
30. McIntosh, J. M. (2000) Toxin antagonists of the neuronal nicotinic acetylcholine receptor, in *Handbook of Experimental Pharmacology. Neuronal Nicotinic Receptors* (Clementi, F., Fornasari, D., and Gotti, C., Eds.) Vol. 144, pp 455−476, Springer-Verlag, Berlin, Germany.
31. Dutertre, S., Nicke, A., and Lewis, R. J. (2005) $\beta2$ subunit contribution to 4/7 α-conotoxin binding to the nicotinic acetylcholine receptor, *J. Biol. Chem. 280*, 30460−30468.
32. Harvey, S. C., and Luetje, C. W. (1996) Determinants of competitive antagonist sensitivity on neuronal nicotinic receptor β subunits, *J. Neurosci. 16*, 3798−3806.
33. Costa, V., Nistri, A., Cavalli, A., and Carloni, P. (2003) A structural model of agonist binding to the $\alpha3\beta4$ neuronal nicotinic receptor, *Br. J. Pharmacol. 140*, 921−931.

BI0611715